Inorg. Chem. **2003**, *42*, 6015–6023

Optical Charge-Transfer in Iron(III)hexacyanoferrate(II): Electro-intercalated Cations Induce Lattice-Energy-Dependent Ground-State Energies

David R. Rosseinsky,*,† Hanyong Lim,†,|| Hongjin Jiang,‡ and Jian Wei Chai§

Singapore Institute of Manufacturing Technology, 71 Nanyang Drive, Singapore 638075, Finisar (Singapore) Pte Ltd., 100 Collyer Quay No. 19-08, Singapore 049315, and Institute of Materials Research and Engineering, 3 Research Link, Singapore 117602

Received September 23, 2002

The maximum of the color-conferring charge-transfer (CT) band in Prussian Blue (PB) varies with the electrochemically introduced cation M^{z+} incorporated (as "supernumerary") for charge neutrality, and the dependence on particular properties of the M^{z+} has been sought. With alkali-metal ions, the CT-maximum shifts are in the same sequence as the PB mass changes on M^+ insertion; the effect on the CT ground state of the intra-lattice interaction of an M^+ with the ferrocyanide CN^- moiety (competing with cation hydration), is then implicated in shifts of the maxima, as the ferrocyanide is the donor center in the optical CT. More definitely, for M^{2+} and Ag^+, solubility-products of the insoluble M^{z+} ferrocyanides (that provide direct indicators of the intra-lattice M^{z+}–$[Fe^{II}(CN)_6]^{4-}$ interactions) show a strong correlation with the spectral shifts. The determining interaction of M^{z+} with ferrocyanide within PB is enhanced in some cases by the accessibility of M^{z+} oxidation states ± 1 different from the common values. PB lattice energies and the ground states of the optical CTs thus appear closely interlinked. The electrochemical uptake of appreciable amounts of the M^{z+} within the lattices was confirmed by XPS.

Introduction

The oft-studied electrochrome Prussian Blue [iron(III)-hexacyanoferrate(II), PB] owes its coloration to the broad intervalence charge-transfer (CT) band centered at ca. 700 nm,[1,2] resulting from the photodriven CT, $Fe^{3+}[Fe^{II}(CN)_6]^{4-} \xrightarrow{h\nu} Fe^{2+}[Fe^{III}(CN)_6]^{3-}$ in the simplest representation. All electrochromes including PB during coloration or bleaching[3] undergo the ionic ingress or egress necessary to maintain lattice electroneutrality during electron injection or expulsion. These counterions (super-numerary,[4] as they are not directly part of the focal chromophore $Fe^{3+}[Fe^{II}(CN)_6]^{4-}$) can be varied electrochemically. The resulting CT spectrum maximum λ_{max} is found[4] to be dependent on the supernumerary if it is an alkali-metal ion, M^+, and it is now found that with some (not all) incorporated M^{2+} supernumeraries, and Ag^+, a substantial shift is observed. These larger shifts imply stronger interactions within the PB lattice than in the M^+ case. The spectroscopy and electrochemistry are presented here, together with a mechanism for the spectrum-determining interactions that link with individual properties of the M^{z+}. XPS was employed to confirm the uptake by PB of the M^{z+}.

An optical CT implies an at-least-minimal preexisting ground-state CT interaction, and for PB the CT band has shown[5] the extent of ground-state delocalization of the transferrable electron to be (only) ~1%, nevertheless contributing toward the PB lattice energy. By contrast, even highly obvious CT bands can accompany negligibly small but necessarily nonzero ground-state contributions to stabilization via delocalization of the transferrable electron.

* Author to whom correspondence should be addressed. School of Chemistry, The University, Exeter EX4 4QD, U.K. E-mail: d.r.rosseinsky@exeter.ac.uk.

† Singapore Institute of Manufacturing Technology.

‡ Finisar (Singapore) Pte Ltd.

§ Institute of Materials Research & Engineering.

|| Current address: Department of Chemical Engineering, Carnegie Mellon University, Pittsburgh, PA 15213-3890.

(1) Mortimer, R. J.; Rosseinsky, D. R. *J. Chem. Soc., Dalton Trans.* **1984**, 2059.

(2) Mortimer, R. J.; Rosseinsky, D. R. *J. Electroanal. Chem.* **1983**, *151*, 133.

(3) Monk, P. M. S.; Mortimer, R. J.; Rosseinsky, D. R. *Electrochromism − Fundamentals and Applications*; VCH Publishers: Cambridge, 1995.

(4) Rosseinsky, D. R.; Glidle, A. *J. Electrochem. Soc*. **2003**, in press.

(5) Mayoh, B.; Day, P. *J. Chem. Soc., Dalton Trans.* **1976**, 1483.

10.1021/ic020575s CCC: $25.00
Published on Web 08/28/2003

The initial PB electrodeposited from an Fe^{3+} $Fe^{III}(CN)_6^{3-}$ solution is[4,6] always the insoluble form $(Fe^{3+})_4[Fe^{II}(CN)_6^{4-}]_3$, iPB, regardless of other M^+ ions in the electrodeposition solution (Cs^+ provides a marked exception[4]). On subsequent CV cycling in M^+-containing solution,[4] M^+ replaces much of the supernumerary Fe^{3+}, the best-incorporated replacement ion being K^+, which if the sole supernumerary gives[3,4] the so-called soluble PB, or sPB, $K^+Fe^{3+}Fe^{II}(CN)_6^{4-}$. M^{2+} cations can similarly be introduced in partial replacement of the initial supernumerary Fe^{3+}.

Experimental Section

Electrochemistry. [In this section, M = mol dm^{-3}.] PB was electrodeposited with a Pt counter-electrode from 1 mM Fe^{3+} (nitrate or chloride) and 1.02 mM $K_3Fe^{III}(CN)_6$ in 10^{-4} M aqueous HNO_3 or HCl solution, in galvanostatic (Solartron 1287) control at 0.1 mA cm^{-2}, on to 20 Ω per square, 1 × 4 cm^2 ITO/glass, from MicroFab Singapore. The ITO, pre-cleaned with ethanol, sonication, and 10-min immersion in 0.1 M HCl, was connected by adhesive copper strip as used for SEM.

Deposited PB after H_2O washing and nitrogen drying was stored for ≥ 30 min in a vacuum desiccator, also after cyclic voltammetry (CV) in M^{z+} solutions, and before spectrophotometry. Except for Pb^{2+} which was the acetate, aqueous M^{2+} solutions for CV comprised 0.2 M sulfates, acting as both background electrolyte and M^{z+} insertion source. [The frequent CV studies of the uptake of KCl by PB accord just the same dual role to that salt]. Analytical grade reagents were used throughout. With Co^{2+} it was established that M^{2+} incorporation ensued regardless of the accompanying anion. Ferric nitrate 0.01 M in 0.01 mM HNO_3 served to produce the Fe^{2+} [in the reductive step], and 0.2 M $AgNO_3$ produced the Ag^+. CVs with regard to SCE were run at 20 mV s^{-1}, for up to 5 cycles.

Spectrophotometry. A PC-driven Ocean Optics USB2000 miniature fiber optic (grating multi-photodiode) spectrophotometer employs optical-fiber leads to samples. Three equally spaced holes in insulation tape on the back of the ITO-glass electrode fixed the PB areas targeted for spectrophotometry. That area near the top of the PB was kept above the CV solution to serve as unaltered-PB absorbance reference. After emersion and drying, the M^{z+}-doped PB was viewed via optical fiber through the second and third holes midway down and near the bottom, respectively. For comparative purposes, the reference spectrum and that for the corresponding M^{z+}-containing PB were normalized so that absorbances at the CT maxima were (both) scaled to unity, and spectra were taken after just one CV cycle to maximize comparabilities between samples. The differences in the normalized spectra, (M^{z+})-PB minus reference, show whether maxima shifts or new maxima extra to the main CT band have been introduced by the inserted M^{z+}.

PB immersed in the Ag^+ solution overnight underwent substantial dissolution, leaving a reddish-purple residue. Another sample (Nafion-coated for stability, hence unsuitable for XPS) after 129 cycles in 0.1 M KCl saturated with AgCl, thus sub-micromolar in Ag^+, acquired a purple tint that was examined spectrophotometrically. The Cu^{2+}-cycled PB was compared with a PB sample electrodeposited in the presence of adventitious Cu^{2+} anodized from a partly uninsulated copper-wire lead.

X-ray Photoelectron Spectroscopy. XPS on the electrodeposited M^{z+}-containing PB was obtained on a VG EscaLab model 220iXL at IMRE Laboratories in Singapore, to confirm that incorporation of the M^{z+} cations within the lattices followed the CV.

Results and Discussion

Electrochemistry: Fundamental Processes. Galvanostatic electrodeposition was preferred in that coulometry allowed nearly exactly reproducible thicknesses essential for comparison purposes. The PB deposits were several microns thick, giving broad thick-layer CV's with substantially displaced cathodic/anodic peaks resulting from the necessary counterion diffusions through the solid. The well rehearsed[1,2,4,6,7] insertion electrochemistry of M^+ supernumeraries after the electrodeposition follow the electrode reactions (where, throughout, the chromophore is written intact, i.e., without fractions or multiples):

$$Fe^{3+}Fe^{III}(CN)_6^{3-} + {}^1/_zM^{z+} + e \rightarrow (M^{z+})_{1/z}Fe^{3+}Fe^{II}(CN)_6^{4-} \quad (1)$$

Because on deposition the M^{z+} is invariably Fe^{3+}, the subsequent bleaching reduction is

$$(Fe^{3+})_{1/3}Fe^{3+}Fe^{II}(CN)_6^{4-} + {}^1/_zM^{z+} + e \rightarrow (M^{z+})_{1/z}(Fe^{3+})_{1/3}Fe^{2+}Fe^{II}(CN)_6^{4-} \quad (2)$$

or

$$(Fe^{3+})_{1/3}Fe^{3+}Fe^{II}(CN)_6^{4-} + {}^4/_{3z}M^{z+} + {}^4/_3e \rightarrow (M^{z+})_{4/3z}(Fe^{2+})_{1/3}Fe^{2+}Fe^{II}(CN)_6^{4-} \quad (2a)$$

then, the (M^{z+})−PB product could be expected to arise from the re-colorizing oxidation:

$$(M^{z+})_{1/z}(Fe^{3+})_{1/3}Fe^{2+}Fe^{II}(CN)_6^{4-} \rightarrow (M^{z+})_{1/z}Fe^{3+}Fe^{II}(CN)_6^{4-} + {}^1/_3Fe^{3+} + e \quad (3)$$

or

$$(M^{z+})_{4/3z}(Fe^{2+})_{1/3}Fe^{2+}Fe^{II}(CN)_6^{4-} \rightarrow (M^{z+})_{1/3z}(Fe^{2+})_{1/3}Fe^{3+}Fe^{II}(CN)_6^{4-} + M^{z+} + e \quad (3a)$$

Analytical results,[4,6] however, show not all supernumerary Fe^{3+} to be replaced in the first cycle (eq 3), but only by a fraction x of about[6] a third or more, hence

$$(M^{z+})_{1/z}(Fe^{3+})_{1/3}Fe^{2+}Fe^{II}(CN)_6^{4-} \rightarrow (M^{z+})_{x/z}(Fe^{3+})_{(1-x)/3}Fe^{3+}Fe^{II}(CN)_6^{4-} + {}^x/_3Fe^{3+} + {}^{(1-x)}/_zM^{z+} + e \quad (4)$$

or if eq 3a pertains, then Fe^{2+}, with no release of supernumerary Fe^{3+}, forms a corresponding part of the Fe supernumerary. The incorporation of the M^{z+} ions in the PB results in the observed spectral changes.

Reduction of aquo-Fe^{3+} in solution around a PB-coated electrode has been shown[2] to take place through PB, preceding any PB reduction in the cathodic limb, as is repeated here, Figure 1a, providing Fe^{2+} for incorporation as supernumerary. (In the galvanostat PB electrodeposition,

(6) Lundgren, C. A.; Murray, R. W. *Inorg. Chem.* **1988**, *27*, 933.

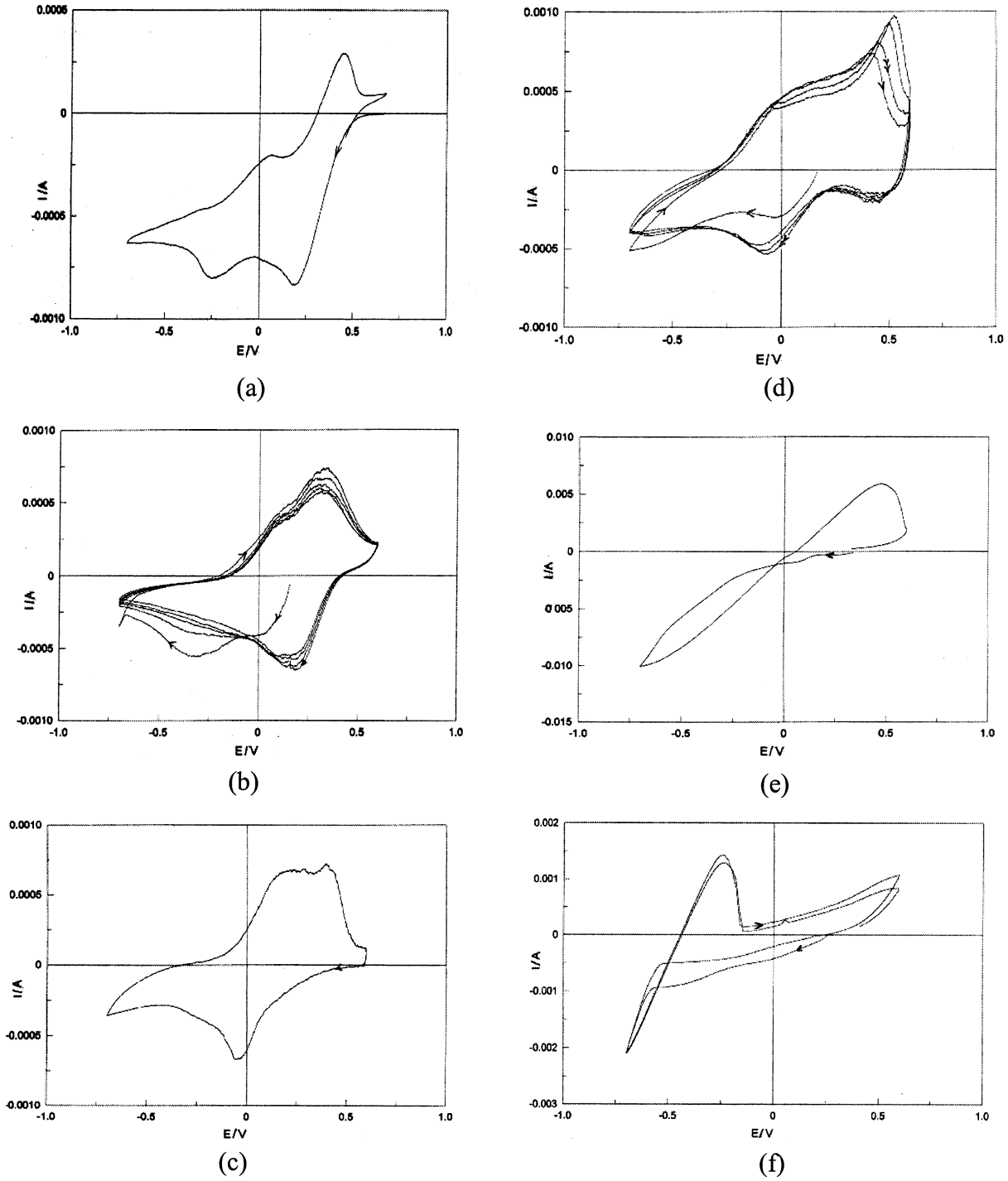

Figure 1. (a) PB CV in Fe^{3+} solution: Fe^{3+} reduction [first trough] followed by [second trough] PB bleaching and Fe^{2+} incorporation. The cathodic electrochemistry involves mainly Fe^{2+} production. Recoloration commences at > 0.25 V. (b) PB cycled in Mg^{2+} solution; first cycle arrowed. First cycle bleaching at −0.3 V; in later cycles at +0.2V, with re-coloration at +0.3 V. (c) PB cycled in Ni^{2+} solution. Bleaching at −0.2 V, recoloration at +0.3V. (d) PB cycled in $CoAc_2$ solution: bleaching with Co^{2+} incorporation and recoloration as in previous figures. (Anodic increments ascribed to anion electrochemistry.) (e) PB cycled in Cu^{2+} solution: curious quasi-ohmic behavior approaching bleach point, ascribed to Cu^{+} or Cu^{0} production, that accompanies the bleaching at −0.4 V. The crossover occurs as a result of Cu^{2+} recovery accompanying recoloration which is complete at +0.5 V. (f) PB cycled in Pb^{2+} solution. Crossover ascribed to Pb^{2+}/Pb^{+} or Pb^{0} processes accompanying PB reduction. Possible Pb^{+} or Pb^{0} participation inferred from the positive current of the reverse limb in the negative-potential range, which indicates reoxidation of an unusual, highly oxidizable, species. Recoloration occurs from + 0.2 V.

the potentials are always between +0.55 V and + 0.35 V, thus never so negative as to produce Fe^{2+} aquo-ion.) Reaction steps 2a and 3a are hence tenable.

Electrochemistry: Specific Cases. A variety of CVs and M^{z+}−PB interactions are inferred below, as is not surprising in view of the wide variety of electron-transfer mechanisms evinced by different redox cations in *homogeneous solution*; here a further complication is introduced by the reactions' being interfacial. As the focus here has been the spectral outcomes, the mechanistic rationalizations are thus provisional. Some of the M^{2+}-incorporating CVs follow that for Mg^{2+}, Figure 1b, Mn^{2+} being so similar as to not need

repetition. The first CV generally had to be taken to −0.5 V, or yet more negative, to complete the bleaching that evidenced the actual M^{z+} insertion; subsequent CVs showed insertion plus bleaching to be possible at less negative potentials, near +0.2 V for Mg^{2+}, and between 0 and −0.2 V for the rest, indicating that the re-structuring inferred[1,6,7] to take place in the first reduction cycle then allows for easier subsequent entry of M^{2+}. To anticipate the XPS results, Mg^{2+} was below detection limits, which indicates that little or no Fe^{z+} (but, doubtless, appreciable water[7]) is lost in the CV cycling, and either the PB bleaching is accompanied by the reduction of supernumerary Fe^{3+} and the uptake of the product Fe^{2+} in its place, accompanied by minimal Mg^{2+} and some H^+ to make up the electroneutrality charge, or Fe^{3+} is substantially returned in a re-coloration reaction

$$(Mg^{2+})_{1/2}(Fe^{3+})_{1/3}Fe^{2+}Fe^{II}(CN)_6^{4-} \rightarrow (Fe^{3+})_{1/3}Fe^{3+}Fe^{II}(CN)_6^{4-} + {}^1/_2Mg^{2+} + e \quad (5)$$

In many cases, continued cycling led to both decreasing adherence of the PB to the electrode, as indicated by the successively diminished CV peaks arising from progressive PB separation from the ITO, plus also an increasing friability of the (originally strongly adherent) PB, and, with Cu^{2+}, shedding of much PB from the electrode. These observations provide direct evidence of the destructive lattice strain that is introduced by insertion of some M^{2+} (in contrast with K^+), buttressing the view that some lattice stabilizing occurs with the wider spread of M^+ counterion charge, contrasting the more concentrated supernumerary charges of M^{2+} or M^{3+}. Arising from the expected variation of the M^{z+}−PB interactions, the width and position of the CV peaks varies with M^{z+}. A second cycle for Ni^{2+} was like the first (Figure 1c), only one trace being recorded. The (Co^{2+})−PB (Figure 1d) shows an early cathodic dip, but decoloration only sets in at ∼ −0.3 V. Arising from the use of di-divalent salts as CV electrolyte, there are large double-layer-reversal currents on polarity change of the applied potential, and the early dips observed here arise from this current. Co^{II} acetate was used in an attempt to lessen the effect, but incremental anodic peaks in Figure 4 ensued, possibly due to the anion; Co^{II} being incorporated as intended in our aims, the anomaly was not pursued.

Cu^{2+} and Pb^{2+} provide some different electrochemistry, as shown in Figure 1, e and f. Both Cu^{2+} and Pb^{2+} lack a clear cathodic peak in the reductive cathodic range, and almost ohmic responses form extreme parts of the trace here. The enhanced M^{2+}−PB interaction of these ions, inferred below, results in a population of closely attached M^{2+} surface cations in the cathodic-range double layer preceding and accompanying the PB reduction, that obviates the usual diffusion-determined response; some electrolyte M^{2+} might, by an adsorption-like interaction, even enter the interstitial channels of the PB before any electron transfer. The displacement of the return limb of the Cu^{2+} at negative potentials, leading to the observed crossover, is attributable to reoxidation[8] of Cu^0 or Cu^+, formed together with PB reduction in the negative-going excursion; interestingly, the ratio of the less-steep to the steeper slope of the linear parts of the cathodic excursion is ∼1:2, implying a 1-electron process followed by a correlated 2-electron process. With Pb^{2+}, also showing a crossover, the remarkable positive peak in the return limb still in the negative-potential range gives evidence of a reoxidation of appreciable intra-lattice Pb^0 or Pb^+ apparently viable at the far end of this range. The recolored PB then examined spectrophotometrically and by XPS thus incorporates the M^{2+} forms of both these supernumeraries. Although further study is of interest, the XPS-assured presence of introduced supernumeraries is sufficient for present purposes.

Table 1. CT λ_{Max} Dependence on Incorporated[a] Closed-Shell M^+

incorporated M^+	Na^+	K^+	Rb^+	Cs^+	ref
λ_{max}/nm	703	686	691	703	4
$(2+\Delta m)/\mu$g cm^{-2}	1.21	0.31	3.72	4.64	10
r/Å	1.02	1.38	1.52	1.67	11
r^{-1}/nm^{-1}	9.8	7.25	6.6	6.0	

[a] Following deposition in K^+ solution, then one cycle in M^+ solution.[4]

Spectroscopic Effects of Incorporated Closed-Shell Cations M^+. The ready exchangeability of supernumerary cations in a CV cycle is presumed to result from the nature of their interstitial sites, with the interstices lying in relatively wide channels of the cubic structure established by Keggin and Miles.[7] (Access to water also ensues: exposure to H_2O vapor within days led to conductivity loss, swelling, and disintegration of bulk sPB compactions, which, when sealed together with silica gel otherwise survived permanently.[9] Our samples, being either fresh or preserved over silica gel, showed no such aqueous decay). The Keggin−Miles structure has recently been confirmed for a number of hexacyanometalates,[10] together with clear illustrations of the accessibility of the channels to incoming supernumeraries.

M^+-dependent λ_{max} values, Table 1, follow in the sequence[28] $Na^+ > K^+ < Rb^+ < Cs^+$. (Data[4,7,8,11,13] for NH_4^+ are also available, but its hydration is unlike that of the M^+.)

This is also the sequence of the PB mass changes Δm (via quartz-microbalance studies[11] before and after a voltammetric cycle in successive M^+ solutions) that is attributed to M^+ gain minus water loss. The sequence is most readily ascribed to the greatest stability[1] of PB−{K^+} (denied the smaller Na^+ by its more tenacious hydration). The strong interaction of K^+ with the intra-PB $Fe^{II}(CN)_6^{4-}$ through the CN^- ligand thereby provides greatest stabilization of the CT ground-

(7) Keggin, J. F.; Miles, F. D. *Nature* **1936**, *137*, 577.
(8) Davies, M. B.; Mortimer, R. J.; Vine, T. R. *Inorg. Chim. Acta* **1988**, *146*, 59.
(9) Rosseinsky, D. R.; Tonge, J. S. *J. Chem. Soc., Faraday I* **1987**, *83*, 245.
(10) Widmann, A.; Kahlert, H.; Petrovic-Prelevic, I.; Wulff, H.; Yakhmi, J. V.; Bagkar, N.; Scholz, F. *Inorg. Chem.* **2002**, *22*, 5706.
(11) Oh, I.; Lee, H.; Yang, H.; Kwak, J. *Electrochem. Commun.* **2001**, *3*, 274.
(12) Shannon, R. D. *Acta Crystallogr.* **1972**, *A32*, 751.
(13) Ruoff, R. S. *J. Phys. Chem.* **1996**, *100*, 8973.
(14) Sillen, L. G.; Martell, A. E. *Stability Constants − Supplement No. 1, Special Publication No. 25*; The Chemical Society: London, 1971; Table 75.
(15) Rosseinsky, D. R. *Chem. Rev.* **1965**, *65*, 467. Rosseinsky, D. R. *Ann. Reports Chem. Soc., A* **1971**, 81.

Table 2. Dependence of $\Delta\lambda_{Max}$ (shifts of λ_{Max} of PB CT Band) on Inserted M^{z+}, Following 1−5 CV Cycles in M^{z+} Solution

M^{z+}	$\Delta\lambda_{max}$/nm[a]	difference-spectrum maxima/nm	*log* K_S/n[b]	n[b]	notes
$Fe^{3+}{}_{uncycled}$	$zero_{uncycled}$	$zero_{uncycled}$			reference spectrum
Mn^{2+}	+19	870(?)[c]	−4.0	3	wide IR band?
Ni^{2+}	−1	(520)	−4.7	3	wk extra band
Co^{2+}	−9	(520)	−5.3	3	wk extra band
Fe^{2+}	−9	(520)	(not available)	3	wk extra band
Cu^{2+}	−11	505	−5.3	3	extra band √
[$Fe^{3+}{}_{uncycled}$	reference		−5.9	7	in (log K_S)/n sequence**]**
Pb^{2+}	−50	565(?)[c]	−6.0	3	solid solution?
Ag^{+}	−51	535	−8.8	5	solid solution
[Ag^{+} salt	(∼ no PB max)	500−540[d]	−		residue from dissolved PB**]**
K^{+}	−25	−	[−2.3][e]	-	ion-pair eqm.
Mg^{2+}	−6	−	[−3.8][e]	-	ion-pair eqm.

[a] With respect to average (reference) spectrum of uncycled samples, $\lambda_{max} = 711 \pm 3$ nm. [b] K_S is the solubility product, listed in log form in refs 16 and 17; n = least (integral) total number of ions comprising $(M^{z+})_{4/z}[Fe^{II}(CN)_6]^{4-}$. [c] Possible artifact from differencing procedure. [d] Read from direct spectrum, Figure 4c. [e] Experimental log K_{DISS} values[17,18] for the ion-pair dissociation equilibrium in H_2O. Calculated[20] difference ≈ 2. (No K_S data available because soluble, no precipitate.)

state, hence the lowest λ_{max}. If K^+, Rb^+, and Cs^+ follow radii r in progressively weaker CN^- interactions, hence ground-state stabilizations, the hitherto unexplained shifts of λ_{max} find a physical rationalization.

The key postulate that is to be the basis for interpreting the spectroscopic sequence then follows: *the ground state of the intervalence CT system is influenced in direct correlation with the lattice energy*, because the Fe^{II} center in the optical CT is just that undergoing the $M^+-Fe^{II}(CN)_6{}^{4-}$ interaction outlined. The ground state of the Fe^{II} is in this view subject to the field of the M^+ as transmitted through the intervening CN^- ion, to an extent governed by the strength of the M^+ interaction. The excited CT state will also experience the M^+ presence, but will a fortiori be the less influenced.

As K^+-containing PB {denoted (K^+)-PB} is the form that ensues if any other (M^+)-PB is in sufficiently long or frequent contact with K^+, all the evidence points to (K^+)-PB being the most stable form of PB, i.e., that with the largest lattice energy U_{latt}. (The extraordinary lengths to which Ludi et al. had to go to avoid K^+ inclusion partly exemplify this.[16]) Hence, the highest energy λ_{max} for (K^+)-PB as shown in Table 1. Thus, simple precepts assist the rationalization of the λ_{max}/M^+ sequence that otherwise lacks any clear physical basis. The postulate underlying the interpretation is supported by wider consideration and further data, as follows.

Spectroscopic Effects of Incorporated Multivalent and Redoxible Cations M^{z+}: *General Considerations.* The average reference value of λ_{max}, that for uncycled (Fe^{3+})-PB, was 711 ± 3 nm, according exactly with λ_{max} for the chloride-solution product,[4] the spread arising inevitably from the approximately flat maximum of the wide CT band with possible superimposed vibrational structure and noise, and some minor PB compositional variation in different electrodepositions. The shifts $\Delta\lambda_{max}$, of λ_{max} for individual (M^{z+})-PB, from the reference value 711 nm, are listed in Table 2. The observed variations should (see preceding section) relate to the interactions of the supernumeraries with the fixed lattice ions, via the −CN of the $Fe^{II}(CN)_6$, and this is endorsed as follows. Individual M^{z+} interactions with $Fe^{II}(CN)_6{}^{4-}$ are well represented by the solubility products K_S for the insoluble M^{z+}-ferrocyanide salts,[17,18] the (fraction-free) formula for each solid comprising n ions.[29] The $^1/_n$ log K_S values for the divalents represent an averaged $M^{z+}-Fe^{II}(CN)_6{}^{4-}$ interaction energy within the solids at comparable hydration energies.[30] These values closely parallel the shifts, $\Delta\lambda_{max}$, in Table 2, and hence support the lattice-energy/ground-state energy correlation postulated for the (M^+)-PB series. Columns 2 and 4 comprise comparable but not equal energies [e.g., the $\Delta\lambda_{max}$ of 50 nm ≙ 12.7 kJ mol^{-1} accompanies a $^1/_n$ RTlog K_S of 34.4 kJ mol^{-1}. However, the latter is not necessarily the actual PB lattice stabilization but an indicator of relativities; were it quantitative the M^{z+} effect on the excited state would still leave $\Delta\lambda_{max} < {}^1/_n\, RT\log K_S$].

The closed-shell M^{z+} (even Ba^{2+} and La^{3+})[18] do not form insoluble ferrocyanides, and the extra lattice energy underlying the insolubility of the ferrocyanides formed by the other M^{2+} (all redoxible in solution) indicates extra lattice interactions of probable CT nature. For the closed-shell M^{z+}, the dissociation constants K_{DISS} for $M^{z+}-$ferrocyanide ion pairs in solution are listed instead in Table 2, opening up an apparent conflict. [Table 2 entries are experimental log K_{DISS} values[17,18] for the ion-pair dissociation equilibrium in H_2O, $\{M^{z+}Fe(CN)_6{}^{4-}\} \rightleftharpoons M^{z+} + Fe(CN)_6{}^{4-}$.] Mg^{2+} is more strongly bound in ion association than is K^+, in accord with the Bjerrum ion-pair[19,20] model, but in apparent contradiction with the present argument relating to $\Delta\lambda_{max}$ values of Mg^{2+} vis-à-vis K^+ involving intra-PB cation/anion interaction. [Fuoss' approximation[21] gives for ion-pair separations a of 5 Å the log K_{DISS} difference of ≈2, from[21] $K_{DISS}{}^{-1} = (3/4\pi a^3 L)\exp(z_+z_-\, e^2/4\pi\epsilon_0\epsilon_r a' k_B T)$.] The XPS actually show little Mg^{2+} uptake, so retained Fe^{z+} could be the culprit.

(16) Ludi, A.; Güdel, H. U. *Struct. Bonding* **1973**, *14*, 1.
(17) Sillen, L. G.; Martell, A. E. *Stability Constants − Supplement No. 1, Special Publication No. 25*; The Chemical Society: London, 1971; Table 10.
(18) Sillen, L. G.; Martell, A. E. *Stability Constants, Special Publication No. 17*; The Chemical Society: London, 1964; Table 10.
(19) Bjerrum, N. *Konink. Dansk. Vidensk. Selsk* **1926**, *7*, 9.
(20) Rosseinsky, D. R. *Comments Inorg. Chem.* **1984**, *3*, 153.
(21) Justice, J. C.; Fuoss, R. M. *J. Phys. Chem.* **1963**, *67*, 1707.

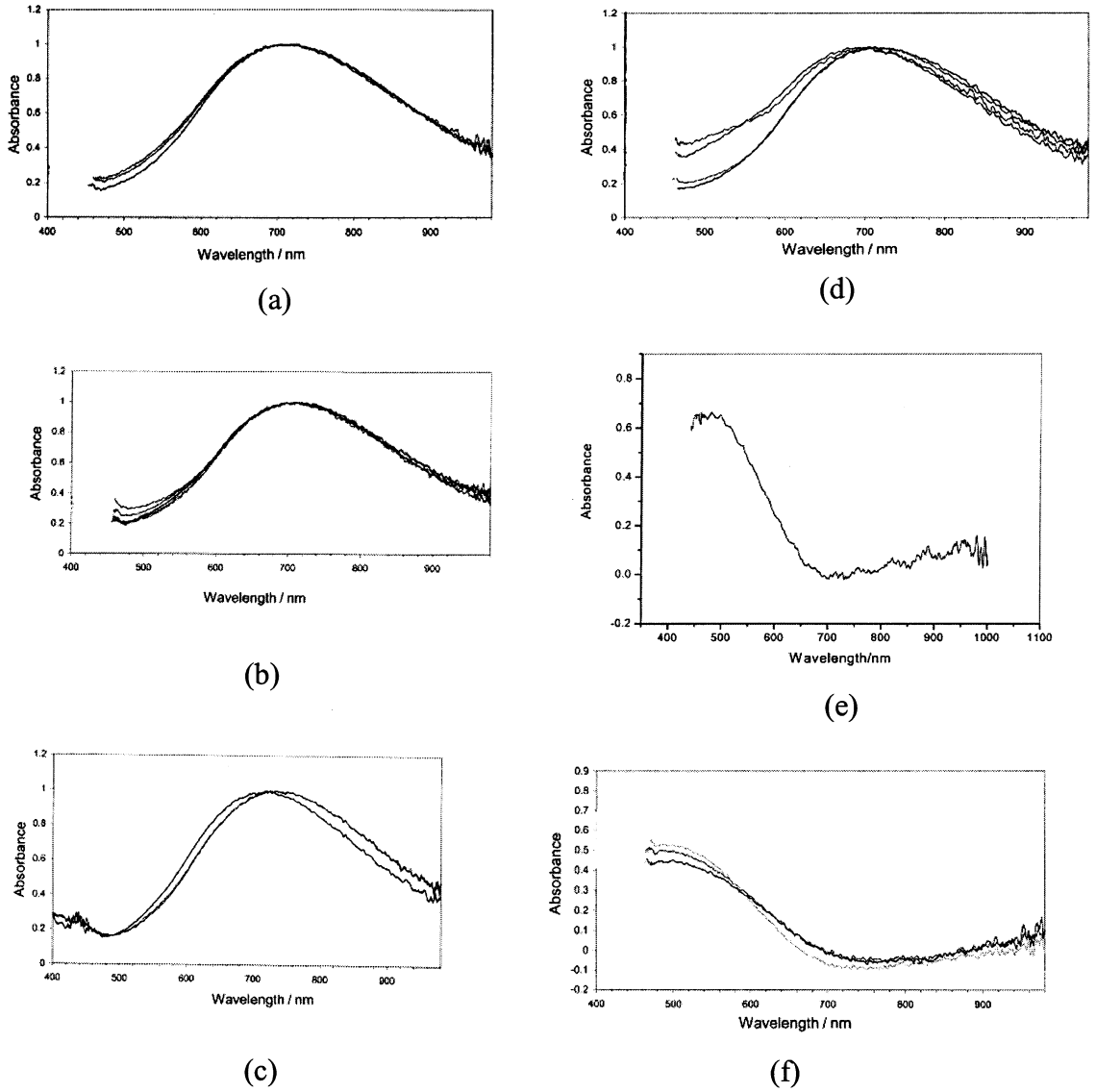

Figure 2. All spectra normalized. (a) Spectra of PB reference (lower curve) and repeated Ni^{2+} curves at the mid and the lower position on the electrode. (b) Four (Mg^{2+})-PB spectra straddling PB reference spectrum: only a small shift evident. (c) PB reference spectrum has the lower-λ maximum; duplicate (Mn^{2+})-PB spectra are shown shifted rightwards. (d) Two (Cu^{2+})-PB spectra showing a kink at 560 nm. Two reference PB spectra (one from Figure b) appear lowermost at low λ, but uppermost at high λ. (e) Difference spectrum, (Cu^{2+})-PB minus PB reference, both normalized; Cu^{2+} incorporated during electrodeposition. (f) Difference spectrum, (Cu^{2+})-PB minus PB reference, both normalized; Cu^{2+} incorporated by CV.

Clearly, examination of K_{DISS} values is less relevant than that of $^1/_n \log K_S$ values.

The supposition that lattice interactions, relative values of which being indicated for M^{z+} by the $^1/_n \log K_S$ values, control the ground-state energy of the optical CT events, seems well supported in general. In further detail, the $\Delta\lambda_{max}$ values of M^{2+} in the range -1 nm (for Ni^{2+}, Figure 2a) to -6 nm (Mg^{2+}, Figure 2b) are attributed to small effects from the diminished cation charges, if there is only weak or no extra absorption in the range 500−570 nm. When $^1/_n \log K_S$ for M^{z+} is more negative than $^1/_n \log K_S$ for the uncycled Fe^{3+}, i.e., < -5.9, the level of interaction becomes marked, in further support of our thesis. Thus for Pb^{2+}, $^1/_n \log K_S$ indicates strong incorporation, and $\Delta\lambda_{max}$ is duly found to be much enhanced. But perhaps even more notably, Ag^+ actually causes dissolution of the iPB, further justifying reliance on the $^1/_n \log K_S$ scale. At the other extreme Mn^{2+} shows an apparently anomalous *positive* $\Delta\lambda_{max}$, hence a case-by-case examination, as follows.

λ_{max} Dependence on Incorporated M^{z+}: Specific Effects. As explained for the electrochemical mechanisms, the spectrophotometric results [cf the variety encountered among homogeneous-solution interactions of different cations, arising from different electron ionisabilities, differing oxidation-state stabilities, hydration effects, size, and the like, all interrelated properties] are again going to be specific to each M^{z+}.

Thus, (i) Mn^{2+}, Figure 2c. Any lattice weakening vis-à-vis (Mg^{2+})-PB, inferred from the positive $\Delta\lambda_{max}$ of (Mn^{2+})-PB, seems discrepant. However, the Mn^{II} state is often oxidizable, and a further CT interaction involving Mn^{III} as optical-CT product in PB could account for the broad difference-spectrum NIR band ($\lambda_{maxNIR?} \approx 870$ nm, Table 2), not seen in the other (M^{2+})-PB. However, superimposition of an extra, broad, NIR absorption onto the central CT band

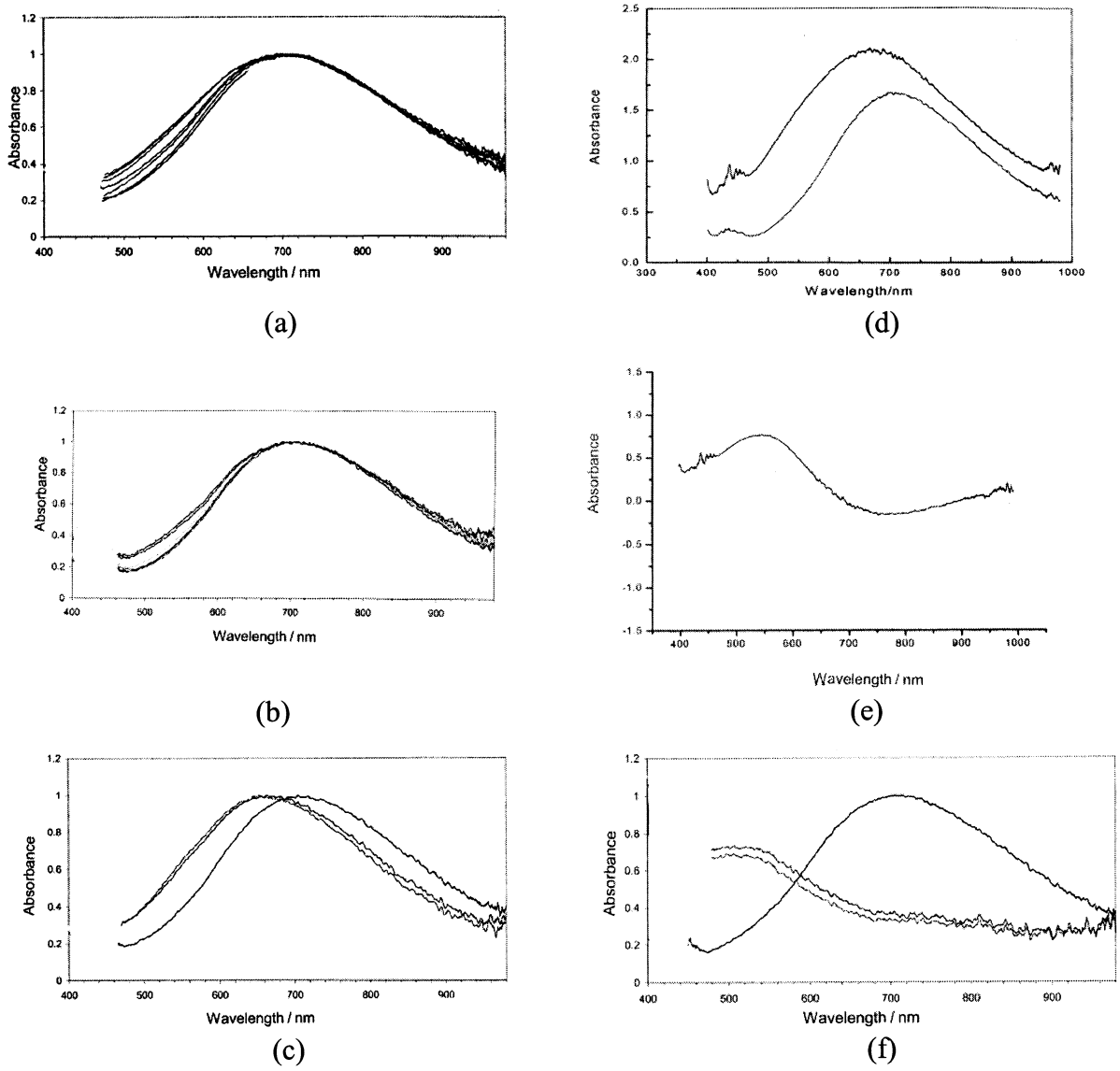

Figure 3. Spectra normalized except (d) and (f). (a) Duplicated (Fe^{2+})-PB spectra with (lowermost) two reference spectra. (b) (Co^{2+})-PB spectra; lowermost: a reference spectrum and a (Co^{2+})-PB trace after a single CV cycle; above this, a repeat reference and uppermost, 4-times cycled (Co^{2+})-PB. (c) Two (Pb^{2+})-PB spectra traces, shifted to lower λ cf the reference PB shown. (d) The (Ag^{+})-PB spectrum (upper) from AgCl in solution, and the PB reference; both are direct spectra. (e) The difference spectrum [normalized, from Figure 3d], for (Ag^{+})-PB. (f) The normalized PB reference spectrum and (lower) the residue from Ag^{+}-dissolved PB (both are the direct spectra).

could shift the net maximum of the latter to longer wavelengths, so accounting for the anomaly. The main CT band may in addition be broadened, as is seen with (Fe^{2+})-PB. The band at ca 450 nm (shown in some spectra) appeared without structure in early PB spectroscopy[1] and relates to an internal $Fe-(CN)_6$ CT absorption not of present interest.

(ii) Fe^{3+}. [All the "reference" spectra on the figures represent the initially deposited Fe^{3+}, the subject of this paragraph.] The "zero" of $\Delta\lambda_{max}$ for the initially deposited iPB apparently conflicts with the -5.9 for the $^1/_n \log K_S$ value, but as only this supernumerary is triply charged, the probably poor charge compensation by M^{3+} vis-à-vis M^{+} and M^{2+} already considered, together with exceptionally enhanced channel water content[11] associated with the 3+ charge, results in a destabilization that invalidates inferences regarding $\Delta\lambda_{max}$ position. Although the $^1/_n \log K_S$ might seem incommensurate with the nil $\Delta\lambda_{max}$, it hence nevertheless provides a useful pointer to the more strongly interacting M^{z+}, and it furthermore indicates relative solubilities such as that seen with Ag^{+}.

(iii) Cu^{2+}. Figure 2d. The (Cu^{2+})-PB is the only transition-metal system here to show an unambiguous new band, at 505 nm, as evidenced by a clear kink in the direct spectrum. The difference spectra, Figure 2 e and f, for Cu^{2+} introduced in electrodeposition and by CV, respectively, demonstrate the new band. Cu^{I}, extant in some stable compounds, could result from optical CT; in aqueous $Cu^{2+}-SO_4^{2-}$ ion association, this accessibility allows quantitative study by spectrophotometry.[22] But the optical CT implies negligible extra ground-state CT stabilization, as K_{DISS} for the $Cu^{2+}-SO_4^{2-}$ ion pair differs little from values for similar $M^{2+}-SO_4^{2-}$ ion pairs that, however, show no optical CT. For the solid (Cu^{2+})-

(22) Hemmes, P.; Petrucci, S. *J. Phys. Chem.* **1968**, *72*, 3986.

PB on the other hand, the somewhat larger $\Delta\lambda_{max}$ and $^1/_n \log K_S$ values predicate an extra, probably CT-enhanced, ground-state interaction. Curiously, part of the PB is shed from the electrode on the first cycle and in further CV.

(iv) Fe^{2+}, Co^{2+}, and Ni^{2+}. Fe^{II} (Figure 3a) is even more readily oxidized than Mn^{II}, so enhanced accessibility of the Fe^{III} state could account for the absence (cf Mn^{II}) of NIR absorption in the <1000-nm range owing to an unobserved >1000 nm NIR absorption in (Fe^{2+})-PB. In contrast, Co^{2+} (Figure 3b) and Ni^{2+} (Figure 2a) are much less easily oxidized ($Co^{II/III}$ involving a spin-state change in thermal reaction), presumably excluding comparable NIR absorption. For these three M^{2+}, if the weak 520 nm bands in the difference spectra involve optical transitions to *lower* oxidation states (feebly emulating (Cu^{2+})-PB), here the modest $\Delta\lambda_{max}$ values indicate little additional ground-state stabilization.

(v) Pb^{2+}. Figure 3c. The large λ_{max} shift is best attributed simply to the strong direct $Pb^{2+}-Fe^{II}(CN)_{6(latt)}$ interaction, of whatever origin, as implied by the $^1/_n \log K_S$ correlation. [The difference spectrum for (Pb^{2+})-PB is of sinewavelike appearance, as would result from differencing two displaced but otherwise identical bands: here a doubtful maximum at 565 nm is accompanied (at meaningless negative absorbance values) by an inverted, approximately mirror-image minimum on the NIR side, and is hence discounted.] The (Pb^{2+})-PB after two cycles remains adherent.

(vi) Ag^+. Figure 3 d, e, and f. The dissolution of PB by Ag^+ solution inhibits extensive analysis, but the purple-tinted product, Figure 3d, obtained from multiple-CV exposure of PB to AgCl dissolved in the contact electrolyte, has allowed a difference spectrum to be obtained, Figure 3e, with a maximum at ~540 nm. As this is close to the range of the additional maximum in the direct spectrum, Figure 3f, for the silver-ferrocyanide/PB residue, a solid solution within PB of silver ferrocyanide is the probable CV product in Figure 3d, again in accord with its large value of $^1/_n \log K_S$ (Table 2).

XPS Results. In the PB samples, all the M^{z+} except Mg^{2+}, which was unexpectedly below detection limits, were present in the XPS at several mol %; the Ag^+ sample was inaccessible (vide supra). The spectra in the M^{z+} regions—except for Pb^{2+}—were multi-peaked and apparently very noisy, prejudicing quantitative assessment; but the multiplicity of peaks observed could well be due to intrinsic variability in the interstitial environments of the M^{z+}. In the structural studies,[10] "... a 'smudgy' position of the potassium ions in the channels of the hexacyano-metalates" is inferred, as is probably applicable to the M^{z+} in our PB samples. For Pb^{2+}, the clear XPS, Figure 4, by contrast confirmed the uniqueness and specificity of the bonding, as expected for the strong interaction imputed to Pb^{2+} in the preceding discussion; a solid solution of $Pb_2\ Fe^{II}(CN)_6$ within PB is again indicated.

CT shift in Modified PB. The λ_{max} of a kind of Prussian Blue containing the pentacyano-aquoiron(II) anion is reported[23] as being shifted 100 nm to longer wavelengths (*cf* that of PB). The weaker average ligand field at the Fe^{II} arising from substitution of an H_2O for a CN^- in part accounts for the lower-energy transition, and furthermore, the 3− anionic charge of the pentacyano-iron(II) ion diminishes the lattice energy cf $Fe^{II}(CN)_6^{4-}$, which would also increase λ_{max}. These considerations add to the view that the CT ground-state energies correlate closely with the lattice energies.

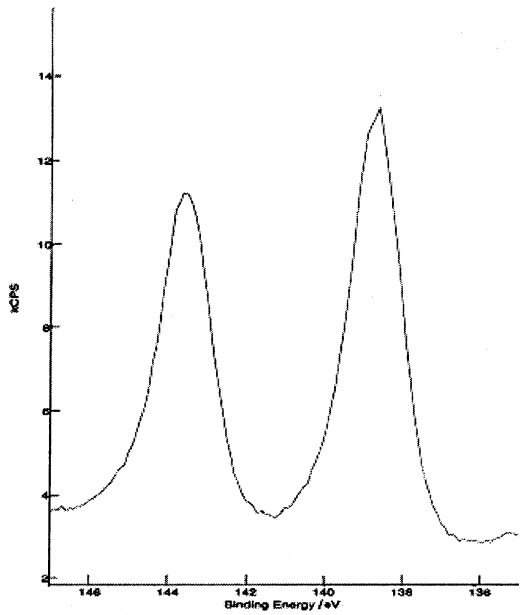

Figure 4. $10^3 \times$ counts s^{-1} versus electron binding energy (BE) in XPS of (Pb^{2+})-PB. Classic normality of $4f_{7/2}$ and $4f_{5/2}$ peaks imply Pb^{2+} sites of uniform environment.

Conclusions

The argument linking the probable lattice-energy consequences of univalent M^+ incorporation in PB with observed shifts of the CT maxima is strongly supported by spectroscopic observations of the effects of M^{2+} and Ag^+ incorporation within PB. The shifts observed in λ_{max} follow the {log(solubility product)}-divided-by-ion-number sequence that provides indicators of the strengths of the M^{z+}-ferrocyanide interaction in the PB lattice: within PB the ground-state energy of the CT participant $Fe^{II}(CN)_6^{4-}$ is clearly influenced by the presence of M^{z+}. The possibility with Cu^{2+} of some additional CT interaction in the lattice energy, the strong interaction with Pb^{2+}, and the strongest interaction with Ag^+ show up both in the shifts of the PB CT maxima and in the solubility−product sequence. The modified-PB λ_{max} also accords with the thesis.

Some precedent for the basis of the present procedure lies in the quantitative rationalization[24,25] of the transition-metal M^{2+} hydration energies in terms of the ligand-field stabilizations inferred from spectroscopy, similarly applied to M^{2+}-halide lattice energies.[26] The present complementary (and less ambitious) approach has been rather to establish cor-

(23) Nechitayilo, V. B.; Styopkin, V. I.; Tkachenko, Z. A.; Goltsov, Y. G.; Sherstyuk, V. P.; Zhilinskaya, W. Z. *Electrochim. Acta* **1995**, *40*, 250.
(24) Dunn, T. M.; McClure, D. S.; Pearson, R. G. *Some Aspects of Crystal Field Theory*; Academic: London, 1965.
(25) Jorgensen, C. K. *Absorption Spectra and Chemical Bonding in Complexes*; M. Dekker: New York, 1962.

relations that confirm a lattice-energy link with observed spectra. Note that U_{latt} is a thermodynamic, bulk quantity, whereas spectral energy states are quantized levels averaged in statistics different from the thermodynamic,[27] but the approximate nature of the present correlations involves little error.

Acknowledgment. We thank Dr. Zhang Xiao (SIMTech) for assistance with electrodeposition, and Dr. R.A. Hann (ICI-Imagedata) for discussing details of the energy correlation. We are indebted to Prof. N. S. Hush (University of Sydney) and Dr. J. Kwak (KAIST, Korea), and Prof. F. Scholz (Ernst Moritz Arndt Universität) for the provision of reprints and preprints. H.Y.L. was a summer intern at SIMTech.

IC020575S

(26) Hush, N. S.; Pryce, M. H. L. *J. Chem. Phys*. **1957**, *26*, 143. Hush, N. S.; Pryce, M. H. L. *J. Chem. Phys*. **1958**, *28*, 244. Hush, N. S. *Discuss. Faraday Soc*. **1958**, *26*, 146.

(27) Hupp, J. T.; Neyhart, G. A.; Meyer, T. J.; Kober, E. M. *J. Phys. Chem*. **1992**, *96*, 10820.

(28) Similar irregularity, in departures from the ionic-radius r_{M^+} sequence, can arise with M^+ properties such as ion-association. Thus, for M^+I^- probed conductometrically,[14] the sequence K < Rb > Cs represents a comparable non-monotony, with a shift in the maximal cation ascribable to aquo-anion specificities. Here anion−cation interaction, basically Coulombic, is in competition with hydration of the cation, H_2O having to be displaced from the cationic hydration shell by the anion, with varying, M^+-dependent, success. In simple molecular models, the cation−anion charge−charge interaction is ∝1/(distance), while the charge−dipole (solvation) interaction ∝1/(distance)^2 is much weaker.[15] From such a model, the $K^+ < Rb^+ < Cs^+$ sequence of λ_{max} is ascribable to progressive weakening of the cation−CN^- interaction with increasing r_{M^+} despite the more rapidly weakening, but feebler, hydration in this sequence.[15] In detail, within the PB lattice, interstitial M^+ will interact with the $Fe^{II}(CN)_6^{4-}$ through the CN^- largely via Coulombic + anion−polarizability interaction, moderated by any H_2O accompanying the M^+, where the H_2O here is deemed to act as dielectric, albeit on a molecular scale.

(29) K_S is the equilibrium constant for $(M^{z+})_{4/z}[Fe^{II}(CN)_6]^{4-}(s) \rightleftharpoons {}^4/_z\, M^{z+} + Fe^{II}(CN)_6^{4-}$, or when $z = 3$ for $(M^{z+})_4([Fe^{II}(CN)_6]^{4-})_3(s) \rightleftharpoons 4M^{z+} + 3Fe^{II}(CN)_6^{4-}$ where the products are aquo-ions. There is a difficulty in directly comparing K_S values for salts with different z values, in that these values refer to equilibria that are written by custom with the lowest integral numbers n of the aquo-ion species. This number differs depending on z, i.e., $n = (1 + 4/z)d$ where d = denominator of any fraction in the parentheses. Thus there are 3 ions in solution from the solid M^{2+} ferrocyanides, whereas for Ag^+ there are 5, and for Fe^{3+} there are 7: the corresponding units are $mol^3\ dm^{-9}$, $mol^5\ dm^{-15}$, and $mol^7\ dm^{-21}$, respectively. Comparison of quantities having different dimensions or units being disallowed, a simple resolution is to divide log K_S by the number (n) of ions involved [giving log-solubility product per ion] which is a rationalizing process both compensating for differing numbers of constituent ions, and conferring the same units, mol dm^{-3}, on all the solubility quantities compared in Table 2. In full, the Table 2 values are thus ${}^1/_n \log \{K_S/(\text{mol dm}^{-3})^n\}$; the K_S are as tabulated in refs 17 and 18, but note that values cited there as K_1, etc. are in fact log K_1, etc.].

(30) Variable in-lattice hydration through the M^{2+} series, weakening the PB-$\{M^{2+}\}$interaction, is partially implicit in the ${}^1/_n \log K_S$ correlation, as K_S, governing the dissolution equilibria, thereby involves the aquo ions.